INTERNATIONAL JOURNAL FOR NUMERICAL METHODS IN FLUIDS
Int. J. Numer. Meth. Fluids 2001; **35**: 173–197

Stratified flow over a backward-facing step: hybrid solution by integral transforms

R. Ramos[a], J. S. Perez Guerrero[b] and R. M. Cotta[c,*]

[a] *Departamento de Engenharia Mecânica, Universidade Federal do Espírito Santo, UFES 29060-970, Vitória, ES, Brazil*
[b] *Comissão Nacional de Energia Nuclear, CNEN/COREJ 22294-900, Rio de Janeiro, RJ, Brazil*
[c] *Programa de Engenharia Mecânica, PEM/COPPE e DEM/EE, Universidade Federal do Rio de Janeiro, UFRJ, Rio de Janeiro, RJ, Brazil*

SUMMARY

The generalized integral transform technique (GITT) is employed in the hybrid numerical–analytical solution of the stratified backward-facing step flow problem, with automatic global accuracy control towards a user-prescribed accuracy target. The present paper is aimed at extending the available database on benchmark results in heat and fluid flow, which were progressively obtained through integral transforms, for the co-validation of more flexible fully discrete approaches. Numerical results are presented for the situations more frequently encountered in the literature Copyright © 2001 John Wiley & Sons, Ltd.

KEY WORDS: integral transforms; Navier–Stokes equations; stratified backward-facing step

1. INTRODUCTION

The research on computer simulation of heat and fluid flow problems is continuously progressing towards the establishment of more robust and precise computational tools, in parallel with dealing with the various challenging new problems posed by the industrial demand for improvement. The literature has been witnessing the proposition of different test problems for the cross-validation of well-known numerical methods, with increasing complexity over the years and with more strict requirements on accuracy achievement. On the other hand, the classical analytical approaches for partial differential equations (PDEs) have been gaining a hybrid numerical–analytical structure, aimed at offering more reliable error control schemes towards the construction of a reference results database, although this is still somehow limited to simplified formulations due to the less flexible analysis required, in comparison with

* Correspondence to: Mechanical Engineering Department, Universidade Federal do Rio de Janeiro, UFRJ EE/COPPE, C.P. 68503, Rio de Janeiro 21945-970, Brazil.

Received July 1999
Revised January 2000

fully discrete approaches. The co-validation of such independent research efforts is a key factor to the mutual progress enhancement and confidence building in these two closely related investigation paths.

One such example of a proposed test problem in heat and fluid flow simulation was motivated by the *Minisymposia on Open Boundary Conditions*, held in Swansea and Stanford, in 1989 and 1991 respectively, when four test cases were defined to challenge the co-validation of numerical procedures [1]. At that occasion, the backward-facing step (BFS) flow problem was solved by Gartling [2] using a finite element procedure and a mesh of 8000 elements, with excellent agreement when compared with experimental works (Dehan and Patrick [3]). More recently, the same problem was solved by Perez Guerrero *et al*. [4] using the generalized integral transform technique (GITT) [5], with a global relative error control of 10^{-4}, yielding full coincidence to four significant digits, at least, against the numerical results of Gartling [2]. Besides, a more thorough comparison with experimental results and previously reported simulations was carried out in Reference [4], exploiting the automatic global accuracy control feature inherent to the hybrid method implemented through integral transforms.

Motivated by such encouraging results, now the goal is to analyse the problem known as the stratified backward-facing step (SBFS), also solved for the same minisymposium by Leone *et al*. [6] through the finite elements method and a mesh of 38400 elements. Here it is handled through the integral transform approach with user-prescribed accuracy. Due to the greater challenge presented by this problem, in the form of a group of eddies situated within strongly recirculating zones, it has deserved closer attention by the international numerical methods community in recent years. Represented by a significant number of publications, such as in Papanastasiou *et al*. [7], who proposed a new outflow boundary condition called a free boundary condition, which is equivalent to extending the validity of the weak form of the governing equations to the synthetic outflow instead of replacing them there with unknown essential or natural boundary conditions. The authors tested this procedure for two different domains: the long domain (truncated to 15 width units with 464 rectangular finite elements) and the short domain (truncated to 7 width units). Also, Kobayashi *et al*. [8] solved the same problem, using the finite volume method and a set of numerical outflow boundary conditions. Manzan and Comini [9], using a streamfunction–vorticity formulation in a finite element implementation, discuss that the inflow and not only the outflow boundary conditions are crucial for a successful modelling of the SBFS problem.

A report about the minisymposium was written by Sani and Gresho [10], where they point out that the actual objective of the event was not fully met. The present work intends to supply additional information from a different point of view on this problem, which means to analytically integral transform the problem in the finite transversal direction and to numerically solve the problem in the infinite longitudinal domain by using an exact scale contraction, which now becomes straightforward when applied to the resulting transformed ordinary differential equation (ODE) system. The hybrid nature of the proposed approach is based on the analytical eigenfunction expansion of the original potentials in one of the space co-ordinates, followed by the integral transformation for elimination of the dependence in this same independent variable. The resulting transformed ODE system in the remaining space co-ordinate is then numerically solved through algorithms for boundary value problems with automatic error control capabilities.

The GITT, as proposed and extended in different sources [4,5,11–20,26,27], is particularly well-suited for benchmarking purposes, such as is intended, in light of its automatic global error control capability, not so easily available in more general purpose fully discrete approaches.

2. PROBLEM FORMULATION

The problem known as the SBFS flow is geometrically defined by two infinite parallel plates between which a Newtonian fluid flows with specified boundary conditions at the inlet and outlet of the channel (Figure 1), with a backward-facing step at the channel entrance. The desired outcome is to find the characteristics of the flow development inside the channel (temperature and velocity fields). Buoyancy effects in the SBFS problem are expected to promote a stratified behaviour in the temperature contours, which are somehow deviated from the expected patterns for a purely diffusive or forced convective situation.

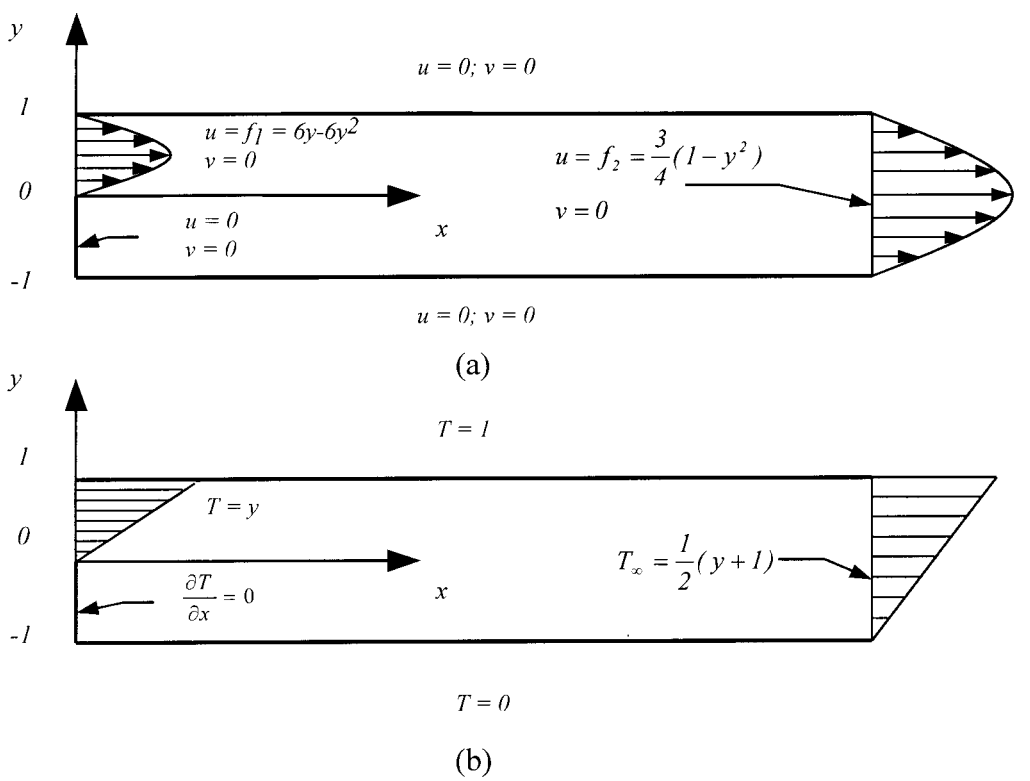

Figure 1. Computational domain and boundary conditions for the flow problem (a) and thermal problem (b).

The mathematical model is formulated once the following assumptions are considered:

- two-dimensional laminar steady flow;
- incompressible flow;
- constant fluid properties, except for the Boussinesq approximation;
- impervious and no-slip walls;
- Newtonian fluid.

The flow inside the duct is governed by the well-known Navier–Stokes and energy equations, which, in terms of streamfunction formulation, are given by

$$\frac{\partial\psi}{\partial y}\frac{\partial^3\psi}{\partial x^3}+\frac{\partial\psi}{\partial y}\frac{\partial^3\psi}{\partial x\,\partial y^2}-\frac{\partial\psi}{\partial x}\frac{\partial^3\psi}{\partial x^2\,\partial y}-\frac{\partial\psi}{\partial x}\frac{\partial^3\psi}{\partial y^3}=\frac{4}{Re}\nabla^4\psi-\frac{16}{Fr}\frac{\partial T}{\partial x} \tag{1}$$

which is valid for $x>0,\ -1<y<1$ and where ∇^4 represents the bi-harmonic operator

$$\nabla^4\equiv\frac{\partial^4}{\partial x^4}+2\frac{\partial^4}{\partial x^2\,\partial y^2}+\frac{\partial^4}{\partial y^4} \tag{2}$$

In the same way, the energy equation in terms of streamfunction formulation becomes

$$\frac{\partial\psi}{\partial y}\frac{\partial T}{\partial x}-\frac{\partial\psi}{\partial x}\frac{\partial T}{\partial y}=\frac{4}{Pe}\left(\frac{\partial^2 T}{\partial x^2}+\frac{\partial^2 T}{\partial y^2}\right) \tag{3}$$

where the streamfunction, $\psi(x,y)$, is defined from the velocity field in the following way:

$$u(x,y)=\frac{\partial\psi(x,y)}{\partial y},\qquad v(x,y)=-\frac{\partial\psi(x,y)}{\partial x} \tag{4a,b}$$

As in previous developments of the GITT in handling flow problems [11–20,26,27], the streamfunction-only formulation is usually preferred; although the method has also been applied several times within the primitive variables formulation. The streamfunction formulation provides the automatic satisfaction of mass conservation and completely eliminates the pressure field from the computations, which would normally act as a source term in the primitive variables choice, sometimes slowing down convergence. On the other hand, the introduction of higher derivatives does not bring in any additional difficulties to the proposed methodology, as will be clear in what follows, and is more closely discussed in Reference [21].

The 12 boundary conditions required to solve Equations (1) and (3) (eight for the flow problem and four for the thermal problem) are specified as follows:

2.1. For the flow problem

—Impervious and no-slip duct walls

$$u(x, -1) = 0; \qquad v(x, -1) = 0, \quad x > 0 \tag{5a,b}$$

$$u(x, 1) = 0; \qquad v(x, 1) = 0, \quad x > 0 \tag{5c,d}$$

which, when represented in terms of the streamfunction, become

$$\psi(x, -1) = k_1; \qquad \frac{\partial \psi(x, -1)}{\partial y} = 0; \qquad \psi(x, 1) = k_2; \qquad \frac{\partial \psi(x, 1)}{\partial y} = 0 \tag{6a–d}$$

where k_1 and k_2 are constants that specify the streamfunction values on the walls.

—Velocity profile is known at the duct entrance

$$u(0, y) = f_1(y); \qquad v(0, y) = 0 \tag{7a,b}$$

Using the streamfunction definition (4) and directly integrating one gets

$$\psi(0, y) = k_1 + \int_{-1}^{y} f_1(\xi)\, \mathrm{d}\xi; \qquad \frac{\partial \psi(0, y)}{\partial x} = 0 \tag{8a,b}$$

—Fully parallel developed flow at $x \to \infty$ (Poiseuille flow)

$$u(\infty, y) = f_2(y) = \frac{3}{2} q(1 - y^2); \qquad v(\infty, y) = 0 \tag{9a,b}$$

or, in streamfunction terms

$$\psi(\infty, y) = k_1 + \left(\frac{3}{2} y - \frac{y^3}{2} + 1\right) q; \qquad \frac{\partial \psi(\infty, y)}{\partial x} = 0 \tag{10a,b}$$

where q is a mass balance coefficient which warrants the continuity satisfaction.

The constant k_2 can be calculated from Equations (8a) or (10a). Using the latter

$$k_2 = k_1 + 2q \tag{11}$$

In this way, the flow problem is formulated just in terms of the streamfunction.

2.2. For the thermal problem

—Known temperatures along the duct walls

$$T(x, -1) = 0; \qquad T(x, 1) = 1 \tag{12a,b}$$

—Known temperature profile and insulated boundary at the duct entrance

$$T(0, y) = y, \quad 0 < y < 1 \tag{13}$$

$$\frac{\partial T(0, y)}{\partial x} = 0, \quad -1 < y < 0 \tag{14}$$

—Thermally fully developed flow at the duct outlet (Poiseuille flow)

$$T(x, y) = T_\infty(y) = \frac{1}{2}(y + 1), \quad x \to \infty \tag{15}$$

3. GITT SOLUTION

To improve computational performance of the method (GITT) [5], it is convenient to perform a boundary conditions homogenization in the co-ordinates to be eliminated through integral transformation. The following analytic filters are then considered:

(a) For the flow problem

$$\psi(x, y) = \phi(x, y) + \psi_\infty(y) \tag{16}$$

where $\psi_\infty(y)$ represents the streamfunction at the fully developed region ($\psi_\infty(y) \equiv \psi(\infty, y)$) and $\phi(x, y)$ is the filtered potential.

(b) For the thermal problem

$$T(x, y) = \theta(x, y) + T_\infty(y) \tag{17}$$

where $T_\infty(y)$ represents the temperature field at the fully developed region ($T_\infty(y) \equiv T(\infty, y)$) and $\theta(x, y)$ is the filtered potential to be determined.

Substituting Equations (16) and (17) into Equations (1) and (3) and also into the boundary conditions (6), (8) and (10) and (12)–(14), one obtains the formulation to be transformed

$$\frac{\partial\phi}{\partial y}\frac{\partial^3\phi}{\partial x^3}+\frac{\partial\phi}{\partial y}\frac{\partial^3\phi}{\partial x\,\partial y^2}-\frac{\partial\phi}{\partial x}\frac{\partial^3\phi}{\partial x^2\,\partial y}-\frac{\partial\phi}{\partial x}\frac{\partial^3\phi}{\partial y^3}+\frac{\mathrm{d}\psi_\infty}{\mathrm{d}y}\frac{\partial^3\phi}{\partial x^3}+\frac{\mathrm{d}\psi_\infty}{\mathrm{d}y}\frac{\partial^3\phi}{\partial x\,\partial y^2}-\frac{\mathrm{d}^3\psi_\infty}{\mathrm{d}y^3}\frac{\partial\phi}{\partial x}$$
$$=\frac{4}{Re}\nabla^4\phi-\frac{16}{Fr}\frac{\partial\theta}{\partial x} \tag{18a}$$

and, for the energy equation

$$\left(\frac{\partial\phi}{\partial y}+\frac{\mathrm{d}\psi_\infty}{\mathrm{d}y}\right)\frac{\partial\theta}{\partial x}-\frac{\partial\phi}{\partial x}\left(\frac{\partial\theta}{\partial x}+\frac{\mathrm{d}T_\infty}{\mathrm{d}y}\right)=\frac{4}{Pe}\left(\frac{\partial^2\theta}{\partial x^2}+\frac{\partial^2\theta}{\partial y^2}\right) \tag{18b}$$

with the required boundary conditions

$$\phi(x,-1)=0;\qquad \frac{\partial\phi(x,-1)}{\partial y}=0;\qquad \phi(x,1)=0;\qquad \frac{\partial\phi(x,1)}{\partial y}=0 \tag{19a–d}$$

$$\phi(0,y)=\int_{-1}^{y}f_1(\xi)\,\mathrm{d}\xi-\left(\frac{3}{2}y-\frac{y^3}{2}+1\right)q;\qquad \frac{\partial\phi(0,y)}{\partial x}=0 \tag{19e, f}$$

$$\phi(\infty,y)=0;\qquad \frac{\partial\phi(\infty,y)}{\partial x}=0 \tag{19g,h}$$

$$\theta(x,-1)=0;\qquad \theta(x,1)=0 \tag{20a,b}$$

$$\theta(0,y)=\frac{1}{2}(y-1),\quad 0<y<1 \tag{20c}$$

$$\frac{\partial\theta(0,y)}{\partial x}=0,\quad -1<y<0 \tag{20d}$$

$$\frac{\partial\theta(x,y)}{\partial x}=0,\quad x\to\infty \tag{20e}$$

Therefore, the problem is now reformulated for the solution of the intermediate functions $\phi(x,y)$ and $\theta(x,y)$.

3.1. Eigenvalue problems

In light of the homogeneous characteristics of the system (18)–(20) in the y-direction, the eigenvalue problems will be chosen in this co-ordinate.

(a) For the flow problem

An eigenvalue problem associated with the homogeneous version of Equation (18a), well detailed in Reference [11] and used in the solution of the Navier–Stokes equations via the GITT [4,5,11–20], is defined as

$$\frac{\mathrm{d}^4 Y_i(y)}{\mathrm{d}y^4} = \mu_i^4 Y_i(y) \tag{21}$$

with boundary conditions

$$Y_i(-1) = 0; \qquad \frac{\mathrm{d}Y_i(-1)}{\mathrm{d}y} = 0; \qquad Y_i(1) = 0; \qquad \frac{\mathrm{d}Y_i(1)}{\mathrm{d}y} = 0 \tag{22a–d}$$

where $Y_i(y)$ and μ_i are the eigenfunctions and eigenvalues associated with the flow problem, which satisfy the following orthogonality property:

$$\int_{-1}^{1} Y_i Y_j \,\mathrm{d}y = \begin{cases} 0, & i \neq j \\ N_i, & i = j \end{cases} \tag{23a,b}$$

and N_i is the norm or normalisation integral.

Equation (21) can be solved analytically, providing a linear combination of trigonometric and hyperbolic functions

$$Y_i(y) = \begin{cases} \dfrac{\cos \mu_i y}{\cos \mu_i} - \dfrac{\cosh \mu_i y}{\cosh \mu_i}, & i = 1, 3, 5, \ldots \\ \dfrac{\sin \mu_i y}{\sin \mu_i} - \dfrac{\sinh \mu_i y}{\sinh \mu_i}, & i = 2, 4, 6, \ldots \end{cases} \tag{24a,b}$$

The eigenvalues are found when the following transcendental equations are solved:

$$\tanh \mu_i = \begin{cases} -\tan \mu_i, & i = 1, 3, 5, \ldots \\ \tan \mu_i & i = 2, 4, 6, \ldots \end{cases} \tag{25a,b}$$

The norm, defined by

$$N_i = \int_{-1}^{1} Y_i^2 \,\mathrm{d}y, \quad i = 1, 2, 3, \ldots \tag{26}$$

presents the following numerical value:

$$N_i = 2, \quad i = 1, 2, 3, \ldots \tag{27}$$

It is convenient to normalize the eigenfunctions for the next steps of the GITT procedure, as

$$\tilde{Y}_i(y) = \frac{Y_i(y)}{N_i^{1/2}} \tag{28}$$

where $\tilde{Y}_i(y)$ represents the normalized eigenfunction.

(b) For the thermal problem
In this case, the chosen eigenvalue problem takes the following form:

$$\frac{\mathrm{d}^2\zeta_i(y)}{\mathrm{d}y^2} + \beta_i^2\zeta_i(y) = 0 \tag{29}$$

with the following boundary conditions:

$$\zeta_i(1) = 0; \qquad \zeta_i(-1) = 0 \tag{30a,b}$$

The solution of this problem results in

$$\zeta_i(y) = \sin[\beta_i(y+1)], \quad i = 1, 2, 3, \ldots \tag{31}$$

where the eigenvalues β_i are calculated from

$$\beta_i = \frac{i\pi}{2}, \quad i = 1, 2, 3, \ldots \tag{32}$$

and in this case, the norm is given by

$$\aleph_i = \int_{-1}^{1} \zeta_i^2(y)\,\mathrm{d}y = 1, \quad i = 1, 2, 3, \ldots \tag{33}$$

3.2. The transformation process

(a) **The flow problem**
The use of the GITT is based on the idea that a function can be represented by an eigenfunction expansion, originated from an auxiliary problem that has information about the diffusion operators of the original partial differential formulation. Thus, it is proposed that, for the flow problem, the function $\phi(x, y)$ can be represented as

$$\phi(x, y) = \sum_{i=1}^{\infty} \bar{\phi}_i(x)\,\tilde{Y}_i(y) \tag{34}$$

where $\bar{\phi}_i(x)$ is the unknown function, which represents the coefficients to be determined in the proposed expansion and depends only on 'x'.

A relation that allows us to define $\bar{\phi}_i(x)$ can be found by invoking the orthogonality property of the eigenfunctions $\tilde{Y}_i(y)$. Operating both members of Equation (34) with $\int_{-1}^{1} \tilde{Y}_i\,\mathrm{d}y$

$$\int_{-1}^{1} \tilde{Y}_i(y)\phi(x, y)\,\mathrm{d}y = \int_{-1}^{1} \tilde{Y}_i(y)\left[\sum_{j=1}^{\infty} \bar{\phi}_j \tilde{Y}_j(y)\right]\mathrm{d}y \tag{35}$$

and reordering in a convenient way

$$\int_{-1}^{1} \tilde{Y}_i(y)\phi(x, y)\,\mathrm{d}y = \sum_{j=1}^{\infty} \bar{\phi}_j \int_{-1}^{1} \tilde{Y}_i(y)\,\tilde{Y}_j(y)\,\mathrm{d}y \tag{36}$$

By the orthogonality property of $\tilde{Y}_i(y)$, it is easily deduced that the terms in the summation of Equation (36) have non-zero values only when $j = i$, so

$$\bar{\phi}_i(x) = \int_{-1}^{1} \tilde{Y}_i(y)\phi(x, y)\,\mathrm{d}y \tag{37}$$

The expression above defines the integral transform for the flow problem, indicating that the original field can be transformed by its internal product with the eigenfunctions. The unknown function is then called the transformed potential, $\bar{\phi}_i(x)$, while Equation (37) is known as the transform formula. Equation (34), which recovers the original potential from the knowledge of the transformed field, is called the inverse formula.

(b) The thermal problem

In the same way, the energy equation can be handled by the following inverse-transform pair

$$\theta(x, y) = \sum_{i=1}^{\infty} \bar{\theta}_i(x)\tilde{\zeta}_i(y) \tag{38}$$

$$\bar{\theta}_i(x) = \int_{-1}^{1} \tilde{\zeta}_i\theta(x, y)\,\mathrm{d}y \tag{39}$$

where $\bar{\theta}_i(x)$ represents the transformed potential and $\tilde{\zeta}_i(y)$ the normalized eigenfunction

$$\tilde{\zeta}_i = \frac{\zeta_i(y)}{\aleph_i^{1/2}} \tag{40}$$

The process of integral transformation of the PDEs (18a,b) into an ordinary differential system begins when the operators $\int_{-1}^{1} \tilde{Y}_i\,\mathrm{d}y$ and $\int_{-1}^{1} \tilde{\zeta}_i\,\mathrm{d}y$ are used on the respective equations making use of the inverse definitions (34) and (38), which will allow us to reorder the terms and to apply the orthogonality properties wherever possible. Then, we find for the flow problem, the following transformed equations:

$$\frac{\mathrm{d}^4\bar{\phi}_i}{\mathrm{d}x^4} + 2\sum_{j=1}^{\infty} D_{ij}\frac{\mathrm{d}^2\bar{\phi}_j}{\mathrm{d}x^2} + \mu_i^4\bar{\phi}_i$$
$$= \frac{Re}{4}\left\{\sum_{j=1}^{\infty}\sum_{k=1}^{\infty}\left[B_{ijk}\frac{\mathrm{d}^3\bar{\phi}_j}{\mathrm{d}x^3}\bar{\phi}_k + C_{ijk}\bar{\phi}_j\frac{\mathrm{d}\bar{\phi}_k}{\mathrm{d}x} - B_{ijk}\frac{\mathrm{d}\bar{\phi}_j}{\mathrm{d}x}\frac{\mathrm{d}^2\bar{\phi}_k}{\mathrm{d}x^2} - A_{ijk}\frac{\mathrm{d}\bar{\phi}_j}{\mathrm{d}x}\bar{\phi}_k\right]\right.$$
$$\left. + \sum_{j=1}^{\infty}\left[A_{\infty ij}\frac{\mathrm{d}^3\bar{\phi}_j}{\mathrm{d}x^3} + B_{\infty ij}\frac{\mathrm{d}\bar{\phi}_j}{\mathrm{d}x} - C_{\infty ij}\frac{\mathrm{d}\bar{\phi}_j}{\mathrm{d}x}\right]\right\} + \frac{16}{Fr}\sum_{j=1}^{\infty} E_{ij}\frac{\mathrm{d}\bar{\theta}_j}{\mathrm{d}x} \tag{41}$$

Applying the same procedure to the energy equation

$$\sum_{k=1}^{\infty}\sum_{j=1}^{\infty} F_{ijk}\bar{\phi}_k\frac{\mathrm{d}\bar{\theta}_j}{\mathrm{d}x} + \sum_{j=1}^{\infty} G_{\infty ij}\frac{\mathrm{d}\bar{\theta}_j}{\mathrm{d}x} - \sum_{k=1}^{\infty}\sum_{j=1}^{\infty} H_{ijk}\frac{\mathrm{d}\bar{\phi}_k}{\mathrm{d}x}\bar{\theta}_j - \frac{\mathrm{d}T_\infty}{\mathrm{d}y}\sum_{k=1}^{\infty} I_{ik}\frac{\mathrm{d}\bar{\phi}_k}{\mathrm{d}x}$$
$$= \frac{4}{Pe}\left(\frac{\mathrm{d}^2\bar{\theta}_i}{\mathrm{d}x^2} - \bar{\theta}_i\beta_i^2\right) \tag{42}$$

where the coefficients can be analytically evaluated from the following integrals:

$$A_{ijk} = \int_{-1}^{1}\tilde{Y}_i\tilde{Y}_j\frac{\mathrm{d}^3\tilde{Y}_k}{\mathrm{d}y^3}\,\mathrm{d}y; \qquad A_{\infty ij} = \int_{-1}^{1}\tilde{Y}_i\tilde{Y}_j\frac{\mathrm{d}\psi_\infty}{\mathrm{d}y}\,\mathrm{d}y \tag{43a,b}$$

$$B_{ijk} = \int_{-1}^{1}\tilde{Y}_i\tilde{Y}_j\frac{\mathrm{d}\tilde{Y}_k}{\mathrm{d}y}\,\mathrm{d}y; \qquad B_{\infty ij} = \int_{-1}^{1}\tilde{Y}_i\frac{\mathrm{d}^2\tilde{Y}_j}{\mathrm{d}y^2}\frac{\mathrm{d}\psi_\infty}{\mathrm{d}y}\,\mathrm{d}y \tag{43c,d}$$

$$C_{ijk} = \int_{-1}^{1}\tilde{Y}_i\frac{\mathrm{d}\tilde{Y}_j}{\mathrm{d}y}\frac{\mathrm{d}^2\tilde{Y}_k}{\mathrm{d}y^2}\,\mathrm{d}y; \qquad C_{\infty ij} = \int_{-1}^{1}\tilde{Y}_i\tilde{Y}_j\frac{\mathrm{d}^3\psi_\infty}{\mathrm{d}y^3}\,\mathrm{d}y \tag{43e,f}$$

$$D_{ij} = \int_{-1}^{1}\tilde{Y}_i\frac{\mathrm{d}^2\tilde{Y}_j}{\mathrm{d}y^2}\,\mathrm{d}y; \qquad E_{ij} = \int_{-1}^{1}\tilde{Y}_i\tilde{\zeta}_j\,\mathrm{d}y \tag{43g,h}$$

$$F_{ijk} = \int_{-1}^{1}\tilde{\zeta}_i\tilde{\zeta}_j\frac{\mathrm{d}\tilde{Y}_k}{\mathrm{d}y}\,\mathrm{d}y; \qquad G_{\infty ij} = \int_{-1}^{1}\tilde{\zeta}_i\tilde{\zeta}_j\frac{\mathrm{d}\psi_\infty}{\mathrm{d}y}\,\mathrm{d}y \tag{43i,j}$$

$$H_{ijk} = \int_{-1}^{1}\tilde{\zeta}_i\frac{\mathrm{d}\tilde{\zeta}_j}{\mathrm{d}y}\tilde{Y}_k\,\mathrm{d}y; \qquad I_{ik} = \int_{-1}^{1}\tilde{\zeta}_i\tilde{Y}_k\,\mathrm{d}y \tag{43k,l}$$

It should be noticed that Equations (41) and (42) present the same non-linear characteristics of the original partial differential system, which are not removed by integral transformation. The same transformation procedure is applied on the boundary conditions (19d–g) and (20c–e), yielding the transformed conditions

$$\bar{\phi}_i(0) = \int_{-1}^{1}\tilde{Y}_i\left[\int_{-1}^{y} f_1(\xi)\,\mathrm{d}\xi - \left(\frac{3}{2}y - \frac{y^3}{2} + 1\right)q\right]\mathrm{d}y \tag{44a}$$

$$\frac{\mathrm{d}\bar{\phi}_i(0)}{\mathrm{d}x} = 0; \qquad \bar{\phi}_i(\infty) = 0; \qquad \frac{\mathrm{d}\bar{\phi}_i(\infty)}{\mathrm{d}x} = 0 \tag{44b–d}$$

$$\sum_{j=1}^{\infty} \left(\frac{\mathrm{d}\bar{\theta}_j(0)}{\mathrm{d}x} L_{ij} + \bar{\theta}_j(0) J_{ij} \right) - K_i = 0 \tag{45a}$$

$$\bar{\theta}_i(\infty) = 0 \tag{45b}$$

where

$$J_{ij} = \int_0^1 \tilde{\zeta}_i \tilde{\zeta}_j \, \mathrm{d}y; \qquad K_i = \int_0^1 \tilde{\zeta}_i (y - T_\infty) \, \mathrm{d}y; \qquad L_{ij} = \int_{-1}^0 \tilde{\zeta}_i \tilde{\zeta}_j \, \mathrm{d}y \tag{46a–c}$$

4. COMPUTATIONAL PROCEDURE

The original partial differential system was transformed into a non-linear ordinary differential system, infinite and coupled, with boundary conditions at two points. This system, composed of Equations (41) and (42), with the boundary conditions (44) and (45), must be solved by numerical procedures, as it is unlikely that analytical solutions may be obtained to this non-linear formulation. One important characteristic of the present approach is the convergence proof for increasing orders of the infinite expansion truncations [5]. This characteristic indicates that it is possible to achieve final solutions with prescribed number of 'exact' (converged) significant digits, under a dynamically determined number of terms in the truncated expansions. The numerical solution of the truncated version of the above ODE system can then be obtained by extensively tested algorithms, available in mathematical sub-routine libraries, such as the IMSL package [22]. This library offers the sub-routine DBVPFD for solving non-linear ordinary differential problems with boundary conditions at two points, including those that may present numerically stiff behaviour, implementing an automatic local error control scheme. The algorithm is based on the PASVA3 [23] routine and makes a discretization over a non-uniform mesh, which is chosen in a way to warrant the same local error at any position. The resulting non-linear algebraic system is solved by the generalized Newton method.

Since all intermediate computational tasks are controlled within the precision limits prescribed by the user, it remains to control the truncation orders for the expansions and, consequently, the ordinary differential system order, to achieve an automatic global error control. The analytical nature of the present technique is then employed, implementing an internal convergence test on the algorithm, at each spatial position where the solution might be desired, through simple formulae such as

$$\varepsilon = \max \left| \frac{\sum_{i=N+1}^{N+\Delta N} \tilde{Y}_i(y)\bar{\phi}_i(x)}{\sum_{i=1}^{N+\Delta N} \tilde{Y}_i(y)\bar{\phi}_i(x) + \psi_\infty(y)} \right| \tag{47}$$

incrementing, by intervals, the number of terms in the expansions truncation, until the ε value above satisfies the requested precision throughout the solution domain. In this way, the algorithm itself controls the final truncation orders necessary to reach the user-prescribed accuracy targets of selected potentials at specified locations.

Another implementation aspect to be discussed is related to the boundary conditions (44c, d) and (45b), which are specified at infinity. In purely numerical methods, this difficulty is normally overcame by considering the boundary conditions to be specified at a position 'far enough' from the origin, until the error introduced by this domain truncation result is insignificant. However, it is not possible to know, *a priori*, if such approximation will affect the final results to within the requested global precision; therefore, it is then unavoidable to solve the problem more than once, taking other domain truncation extents and verifying if a certain convergence criterion is satisfied.

This difficulty is easily avoided by the present method using a scale contraction of the independent variable x, redefining the domain from $[0, \infty]$ to $[0, 1]$. The exact domain contraction here considered was

$$\eta = 1 - \mathrm{e}^{-cx} \tag{48}$$

where c is a scale compression parameter, which provides

$$\frac{\mathrm{d}\eta}{\mathrm{d}x} = c(1 - \eta) \tag{49}$$

Thus, the problem is now solved in the contracted independent variable domain, with the boundary conditions at infinity now exactly specified at $\eta = 1$.

5. RESULTS AND DISCUSSIONS

As previously mentioned, the present approach was employed in the solution of the problem proposed on the occasion of the *Minisymposium on Open Boundary Conditions* [1], first analysed by Leone [6] and revisited by Papanastasiou *et al.* [7], Kobayashi *et al.* [8], and Mazan and Comini [9]. Thus, the values of Reynolds, Froude and Peclet numbers were chosen as equivalent to those in the cited investigations, which yields $Re = 1600$, $Fr = 56.89$ and $Pe = 1600$, considering the present definition of these parameters. Taking the Prandtl number equal to unity ($Pr = 1.0$), the Grashoff number becomes $Gr = 4.5 \times 10^4$, which results in the same value for the Rayleigh number, $Ra = 4.5 \times 10^4$.

Table I. Convergence analysis of longitudinal velocity component, $u(x, y)$.

NV = NT (CPU, s)	$x = 6.0$	$x = 14.0$	$x = 30.0$
$u(x, -0.9)$			
4 (4.)	0.2482	−0.0699	0.1071
8 (26.)	0.3559	−0.0491	0.1117
12 (64.)	0.3762	−0.0502	0.1115
16 (317.)	0.3755	−0.0498	0.1110
20 (223.)	0.3727	−0.0496	0.1110
24 (834.)	0.3715	−0.0496	0.1110
28 (1218.)	0.3711	−0.0496	0.1110
$u(x, -0.5)$			
4	1.211	0.1071	0.5278
8	1.230	0.0961	0.5366
12	1.235	0.1027	0.5358
16	1.234	0.1010	0.5346
20	1.232	0.1006	0.5346
24	1.232	0.1005	0.5346
28	1.232	0.1005	0.5346
$u(x, 0.0)$			
4	0.7737	0.9110	0.8434
8	0.6833	0.9016	0.8411
12	0.6722	0.9066	0.8409
16	0.6723	0.9048	0.8409
20	0.6736	0.9042	0.8409
24	0.6741	0.9040	0.8409
28	0.6743	0.9040	0.8408
$u(x, 0.5)$			
4	−0.0627	0.9454	0.5377
8	−0.0330	0.9370	0.5296
12	−0.0475	0.9329	0.5305
16	−0.0431	0.9355	0.5316
20	−0.0438	0.9359	0.5316
24	−0.0433	0.9360	0.5316
28	−0.0434	0.9360	0.5316
$u(x, 0.9)$			
4	−0.0430	0.1899	0.1103
8	−0.0322	0.2169	0.1084
12	−0.0356	0.2017	0.1088
16	−0.0365	0.2036	0.1094
20	−0.0365	0.2048	0.1094
24	−0.0363	0.2052	0.1094
28	−0.0363	0.2053	0.1094

A computational code was written in FORTRAN77, running on a PC Pentium 266 MHz/64 Mb, with a relative error target of 10^{-3}, with the convergence controlled to within ± 1 in the third significant digit of the longitudinal velocity component, $u(x, y)$. The CPU time spent in

the worst case analysed, which required truncation orders in the two expansions of NV = NT = 28 was, approximately, 1200 s. The performance of the ODEs system solver (sub-routine DBVPFD) was considerably enhanced by implementing a preliminary search for a more

Table II. Convergence analysis of temperature field, $T(x, y)$.

NV = NT	$x = 6.0$	$x = 14.0$	$x = 30.0$
$T(x, -0.9)$			
4	0.0794	0.0269	0.0562
8	0.1117	0.0279	0.0559
12	0.1193	0.0292	0.0558
16	0.1194	0.0290	0.0557
20	0.1193	0.0288	0.0557
24	0.1194	0.0288	0.0557
28	0.1194	0.0288	0.0557
$T(x, -0.5)$			
4	0.3813	0.1136	0.2640
8	0.4029	0.1169	0.2671
12	0.4088	0.1187	0.2670
16	0.4082	0.1181	0.2667
20	0.4072	0.1179	0.2667
24	0.4071	0.1178	0.2667
28	0.4070	0.1178	0.2667
$T(x, 0.0)$			
4	0.7957	0.3276	0.4969
8	0.8017	0.3250	0.5005
12	0.8031	0.3272	0.5003
16	0.8030	0.3266	0.4999
20	0.8025	0.3264	0.4999
24	0.8023	0.3264	0.4999
28	0.8022	0.3264	0.4999
$T(x, 0.5)$			
4	0.9576	0.6558	0.7313
8	0.9315	0.6520	0.7325
12	0.9390	0.6553	0.7324
16	0.9389	0.6545	0.7320
20	0.9388	0.6542	0.7320
24	0.9390	0.6542	0.7320
28	0.9389	0.6542	0.7320
$T(x, 0.9)$			
4	0.9789	0.9249	0.9427
8	0.9803	0.9149	0.9442
12	0.9852	0.9211	0.9442
16	0.9858	0.9205	0.9441
20	0.9857	0.9202	0.9441
24	0.9857	0.9201	0.9441
28	0.9857	0.9201	0.9441

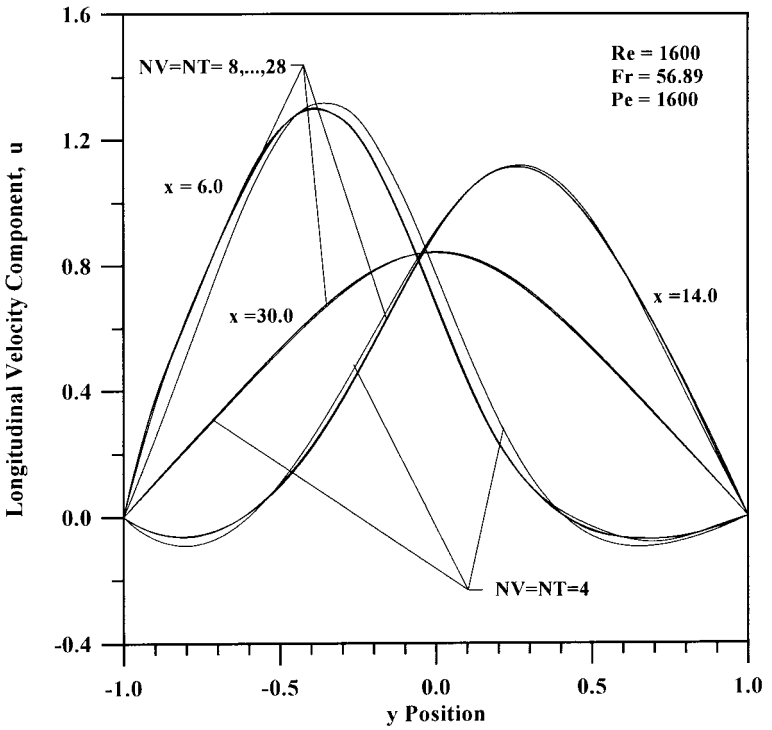

Figure 2. Convergence analysis of longitudinal velocity component profiles, $u(x, y)$.

adequate initialization spatial mesh, obtained with increasing values of the governing parameters and lower truncation orders ($NV = NT = 4$, starting with $Re = Pe = 100$), so as to identify the recirculation regions along the x co-ordinate. The parameter of scale compression, c, also has to be suitably chosen for a successful numerical integration of the ODEs system, and in the present problem ranges from $c = 0.1$, for $Re = Pe = 100$, to $c = 0.0016$ for $Re = Pe = 1600$.

The history of the present eigenfunction expansion convergence process is illustrated in Table I, for the longitudinal component of velocity, u, and Table II, for the temperature field, T, and also represented to a graphical scale in Figures 2 and 3 respectively for x values of interest selected from the literature.

From Table I it is observed that all velocity component values listed are converged up to $NV = NT = 24$, to within the third significant digit (considering the error control of ± 1 in the third significant digit), and in various positions even to within the fourth digit at lower truncation orders. The convergence in the position $x = 30$ completely occurs at truncation orders less than $NV = NT = 8$, since positions next to the fully developed flow region are expected to experience a faster convergence rate, once the filter chosen in Equation (16) more closely reproduces the behaviour in this region. The required CPU time for each individual truncation order run is shown between brackets right after the first column of Table I. It is

interesting to note that it is possible to obtain graphical convergence, including the reproduction of the recirculation zones, with enough accuracy for most engineering purposes, at quite low truncation orders (for instance, NV = NT = 8) and consequently very low computational effort (CPU time of 26 s only).

In the same way, full convergence to the third significant digit of the temperature field is observed in Table II, with truncation orders as low as NV = NT = 8, in a general way. Notable exceptions occur for $T(6, -0.9)$, which converged around NV = NT = 16, and $T(6, 0.9)$ (convergence around NV = NT = 20). Such behaviour is explained by the fact that, in the inlet region of the channel where there is a strong recirculation zone, the proposed filter is not effective in the reduction of the equations source terms importance, specially in positions very close to the walls, as indicated by the quoted co-ordinates. This behaviour can be better observed through Figures 2 and 3 for the graphical convergence illustration. To the graphical scale, the results are essentially converged to much lower truncation orders than those pointed out in the above discussions for the tabulated results.

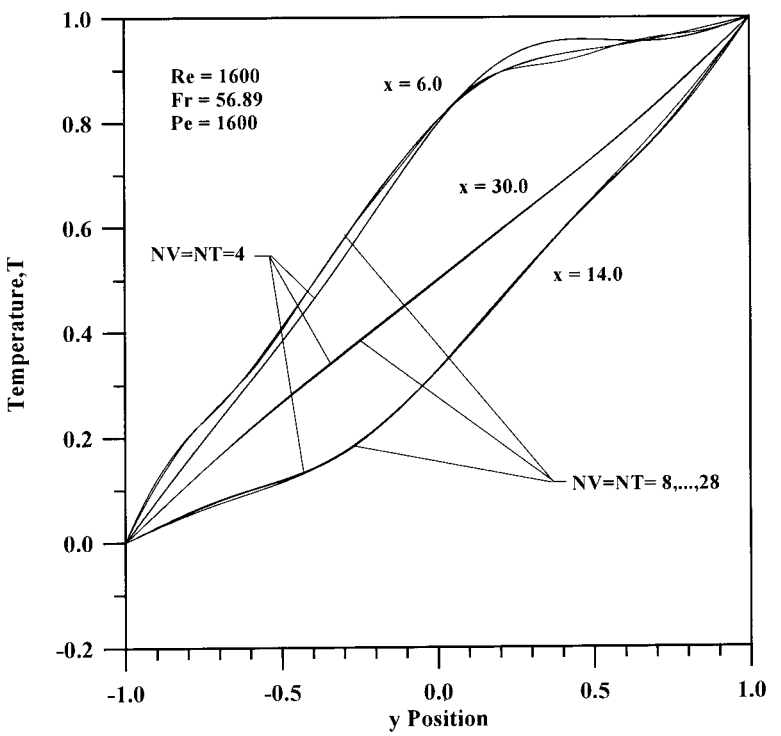

Figure 3. Convergence analysis of temperature profiles, $T(x, y)$.

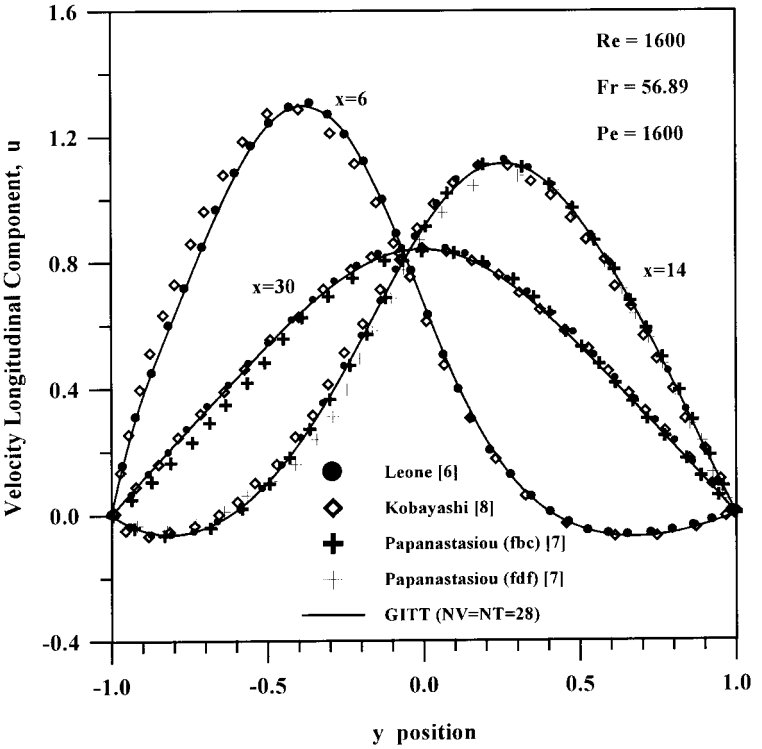

Figure 4. Comparison of longitudinal velocity component profiles, $u(x, y)$.

Comparisons with literature data can be seen in Figures 4–7, where the good agreement between the results from different sources for the longitudinal velocity component, u, the temperature profiles, T, transversal velocity component, v, and the streamfunction, ψ, respectively, is noticed. The best overall agreement is offered by the present integral transform results and the finite elements simulation of Leone [6], and the most significant deviations are observed in the finite volumes simulation of Kobayashi *et al.* [8], especially for the transversal velocity component profiles. Tabulated results were not readily available for a direct numerical comparison.

Longitudinal steady state profiles of u, T and ψ are presented in Figures 8–11 respectively, where the five eddies, expected from the solution of this problem, can be clearly observed. These qualitative behaviours are in excellent agreement with the reference solution proposed by Leone [6]. In Figure 10, the temperature contour map is plotted, which demonstrates the thermally stratified behaviour of the problem. Also shown in Figure 11, is the evolution of the steady state contours of the streamfunction as $Re = Pe$ is gradually increased (with the

corresponding variation of the Grashoff number), illustrating the progressive appearance of further recirculation zones in the steady state flow structure.

6. CONCLUSIONS

The integral transform solution of the stratified flow over a backward-facing step is described in detail, including the analytical derivations and the computational implementation. Numerical results are obtained for the test case previously considered in the open literature, and a thorough convergence analysis is presented in different regions of the solution domain. The fully converged results thus achieved provide a set of tabulated benchmark results for future comparisons, while previously reported simulations are critically examined against the error-controlled integral transform results, to a graphical scale.

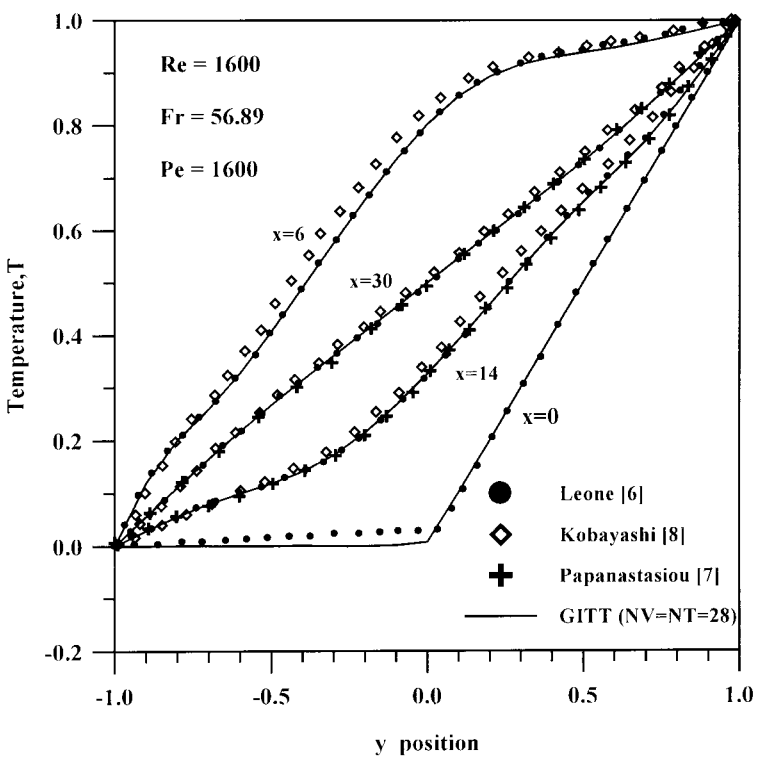

Figure 5. Comparison of temperature profiles, $T(x, y)$.

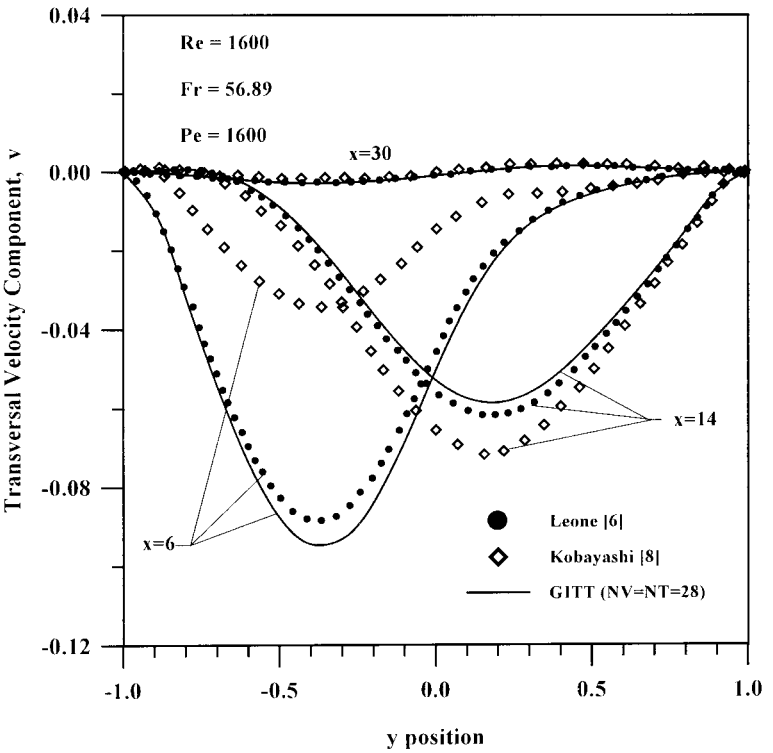

Figure 6. Comparison of transversal velocity component profiles, $v(x, y)$.

The present approach may also be extended to include three-dimensional effects, following recent developments on this technique, either directly in the primitive variables formulation [24] or by employing the vector/scalar potentials formulation, as considered in Reference [15,20] for cavity flow problems. In general, this type of approach is associated with disadvantages related to an excessive analytical involvement and derivation effort, in contrast to purely discrete methods. However, the new generation of mixed symbolical–numerical computation platforms, as the Mathematica package [25] here employed for checking purposes, has been permitting the elimination of this apparent difficulty for more wide spread use of analytical-based techniques such as the one here advanced [20,26,27].

Recent developments on the GITT approach [13–20] shall allow for the extension of this research towards the inclusion of additional effects and phenomena, such as turbulence, irregular geometries, three-dimensional effects, transient regime, variable physical properties, etc., aimed at offering a more complete co-validation basis to the numerical methods community in heat and fluid flow.

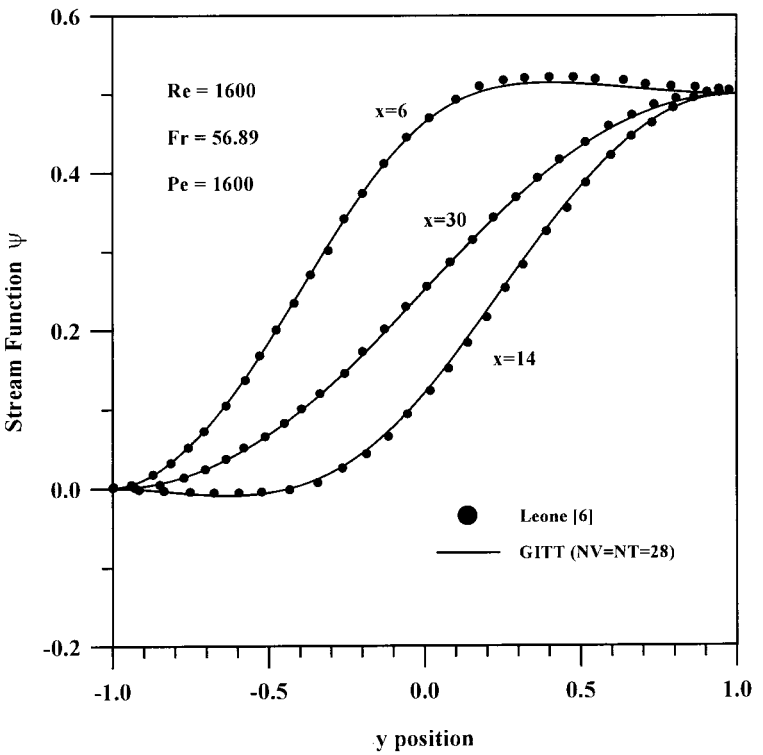

Figure 7. Comparison of streamfunction profiles, $\psi(x, y)$.

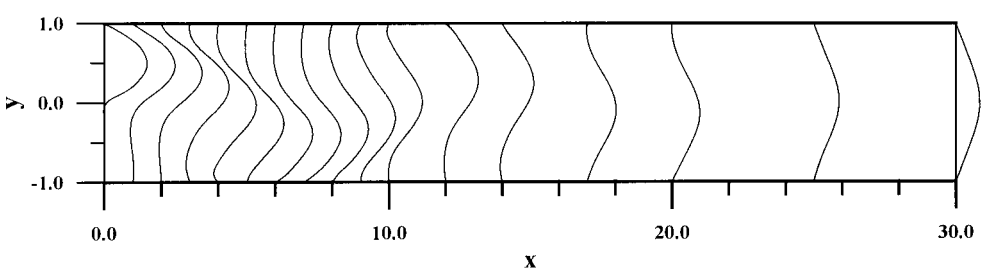

Figure 8. Longitudinal $u(x, y)$ profiles along the channel ($Re = 1600$, $Fr = 512/9$, $Pe = 1600$).

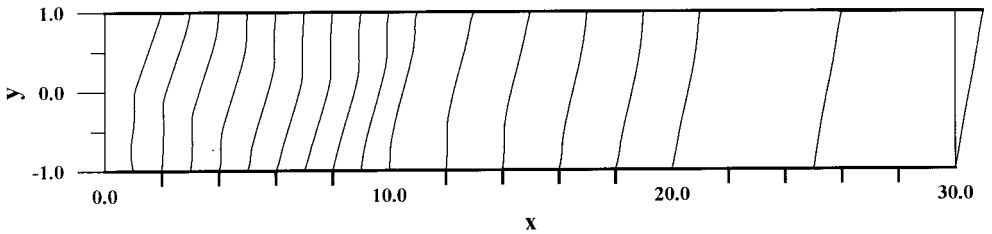

Figure 9. Longitudinal temperature profiles along the channel ($Re = 1600$, $Fr = 512/9$, $Pe = 1600$).

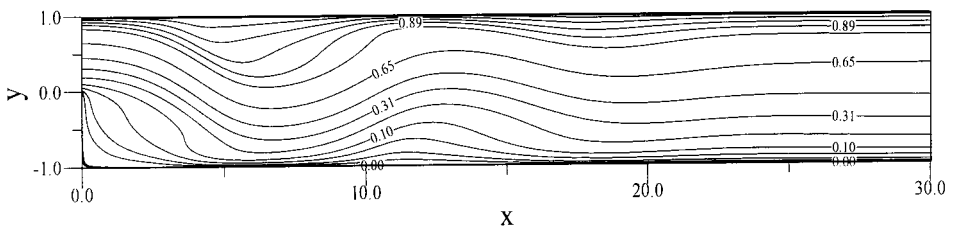

Figure 10. Temperature contours ($Re = 1600$, $Fr = 512/9$, $Pe = 1600$).

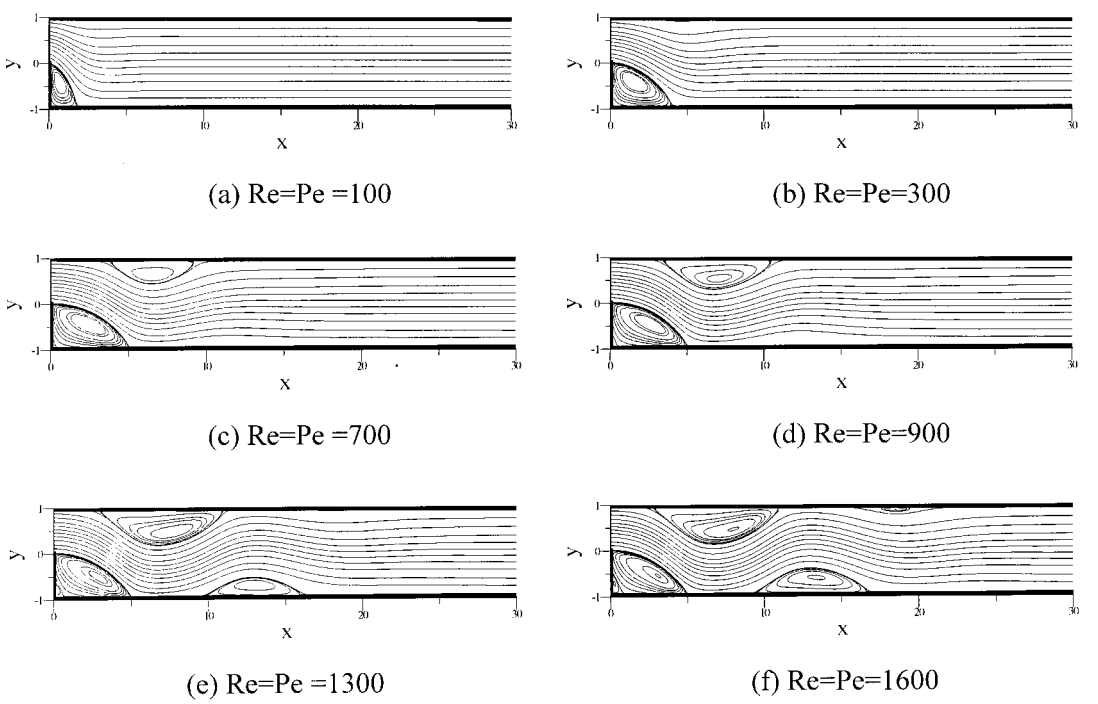

Figure 11. Evolution of steady state contours of the streamfunction ($Fr = 512/9$).

ACKNOWLEDGMENTS

This paper was motivated by the *Minisymposia on Open Boundary Conditions*, held in Swansea and Stanford, in 1989 and 1991. The authors would like to acknowledge the financial support provided by CAPES, CNPq and FUJB, all of them federal sponsoring agencies in Brazil. Also, Dr R. Ramos would like to acknowledge the kind hospitality and support of Prof. Roland W. Lewis and of the Department of Civil Engineering, University College of Swansea, U.K., during his one-year stay in Swansea, when a good portion of the present work was completed.

APPENDIX A. NOMENCLATURE

A, B, C, D, E, F, G, H, I, J, K, L, M, N	transformation coefficients obtained in the streamfunction and temperature integral transformation process
b	half spacing between parallel plates
c	scale compression parameter
D_h	hydraulic diameter, $D_h = 4b$
f_1	longitudinal velocity component distribution at the channel inlet
Fr	Froude number, $Fr = (U/u_B)^2$, where $u_B = (\gamma g \Delta T / H^{1/2})H$
g	modulus of the gravity vector
Gr	Grashoff number, $Gr = Re^2/Fr$
H	channel height
N_i, $\aleph_i$	streamfunction and temperature eigenfunctions norms respectively
NV, NT	truncation orders of streamfunction and temperature expansions respectively
p	pressure, $p = p^*/\rho U$
Pe	Peclet number, $Pe = Re \cdot Pr$
Pr	Prandtl number, $Pr = \nu/\alpha$
q	mass balance coefficient ($q = 1/2$, for the present definitions of f_1 and f_2)
Q, R, S, V, Z	transformation coefficients obtained in the boundary conditions integral transformation process
Ra	Rayleigh number, $Ra = Pr \cdot Gr$
Re	Reynolds number, $Re = 4Ub/\nu$
T	temperature, $T = (T^* - T^*_{\text{bottom}})/(T^*_{\text{top}} - T^*_{\text{bottom}})$
u	longitudinal velocity component, $u = u^*/U$
U	mean velocity
v	transversal velocity component, $v = v^*/U$
x, y	longitudinal and transversal coordinates respectively, $x = x^*/b$, $y = y^*/b$

Greek letters

α	thermal diffusivity

β_i	temperature eigenvalues
γ	volumetric expansion coefficient
ε	global error control parameter
ϕ	filtered streamfunction
η	domain contraction variable
ζ_i	temperature eigenfunctions
μ_i	streamfunction eigenvalues
ψ	streamfunction

Subscripts and superscripts

i, j, k, l, m, n	order of eigenquantity
∞	indicates parameter, coefficient, velocity or temperature related to $x \to \infty$
—	integral transformed quantity
$\sim$	normalized quantity
*	dimensional variable

REFERENCES

1. Announcement. Open Boundary Condition (OBC) Minisymposium. *International Journal for Numerical Methods in Fluids* 1990; **11**: 952.
2. Gartling DK. A test problem for outflow boundary conditions—flow over a backward facing step. *International Journal for Numerical Methods in Fluids* 1990; **11**: 969–984.
3. Dehan MK, Patrick MA. Laminar flow over a downstream-facing step in a two-dimensional flow channel. *Transactions of the Institute of Chemical Engineers* 1974; **52**: 361–367.
4. Pérez Guerrero JS, Cotta RM. Benchmark integral transform results for flow over a backward-facing step. *Computers and Fluids* 1996; **25**: 527–540.
5. Cotta RM. *Integral Transforms in Computational Heat and Fluid Flow*. CRC Press: Boca Raton, FL, 1993.
6. Leone JM Jr. Open boundary condition symposium benchmark solution: stratified flow over a backward-facing step. *International Journal for Numerical Methods in Fluids* 1990; **11**: 969–984.
7. Papanastasiou TC, Malamataris N, Ellwood K. A new outflow boundary condition. *International Journal for Numerical Methods in Fluids* 1992; **14**: 587–608.
8. Kobayashi MH, Pereira JCF, Sousa JMM. Comparison of several open boundary numerical treatments for laminar recirculating flows. *International Journal for Numerical Methods in Fluids* 1993; **16**: 403–419.
9. Manzan M, Comini G. Inflow and outflow boundary conditions in the finite element solution of the streamfunction–vorticity equations. *Communications in Numerical Methods in Engineering* 1995; **11**: 33–40.
10. Sani RL, Gresho PM. Résumé and remarks on the Open Boundary Condition Minisymposyum. *International Journal for Numerical Methods in Fluids* 1994; **18**: 983–1008.
11. Pérez Guerrero JS, Cotta RM. Integral transform method for Navier–Stokes equations in streamfunction-only formulation. *International Journal for Numerical Methods in Fluids* 1992; **15**: 399–409.
12. Pérez Guerrero JS, Cotta RM. Integral transform solution of developing laminar duct flow in Navier–Stokes formulation. *International Journal for Numerical Methods in Fluids* 1995; **20**: 1203–1213.
13. Lima JA, Pérez Guerrero JS, Cotta RM. Hybrid solution of the averaged Navier–Stokes equations for turbulent flow. *Computational Mechanics* 1997; **19**(4): 297–307.
14. Leal MA, Cotta RM. Steady and transient integral transform solutions of natural convection in enclosures. In *Proceedings of the ICHMT International Symposium on Computational Heat Transfer*, de Vahl Davis G (ed.). Begell House: Turkey, 1997; 418–432.

15. Quaresma JNN, Cotta RM. Integral transform method for the Navier–Stokes equations in steady three-dimensional flow. In *Proceedings of the Tenth ISTP–International Symposium on Transport Phenomena*, Kyoto, Japan, November, Suzuki K (ed.), 1997; 281–287.
16. Pereira LM, Pérez Guerrero JS, Cotta RM. Integral transformation of the Navier–Stokes equations in cylindrical geometry. *Computational Mechanics* 1998; **21**(1): 60–70.
17. Leal MA, Pérez Guerrero JS, Cotta RM. Natural convection inside two-dimensional cavities—the integral transform method. *Communications in Numerical Methods in Engineering* 1999; **15**: 113–125.
18. Pérez Guerrero JS, Quaresma JNN, Cotta RM. Simulation of laminar flow inside ducts of irregular geometry using integral transforms. *Computational Mechanics* 2000; **25**: 413–420.
19. Machado HA, Leal MA, Cotta RM. A flexible algorithm for transient thermal convection problems via integral transforms. In *Proceedings of the International Symposium on Computational Heat and Mass Transfer*, North Cyprus, Turkey, Mohamad AA (ed.), April, 1999; 13–31.
20. Cotta RM. *The Integral Transform Method in Thermal and Fluids Science and Engineering*. Begell House: New York, 1998.
21. Figueira da Silva E, Cotta RM. Mixed convection within vertical parallel plates: hybrid solution by integral transforms. *Numerical Heat Transfer Part A* 1998; **33**: 85–106.
22. IMSL library. Math/Lib: Houston, TX, 1989.
23. Pereyra V. PASVA3: an adaptative finite-difference FORTRAN program for first order non linear boundary value problems. In *Lecture Notes in Computer Science*, vol. 76. Springer: Berlin, 1978; 67–88.
24. Pereira LM, Pérez Guerrero JS. An alternative solution to the Navier–Stokes equation in primitive variables via integral transform. In *V North–Northeast Mechanical Engineering Congress—CEM-NNE 98*, ABCM/Brazil (ed.), 1998; 620–627, in Portuguese.
25. Wolfram S. *The Mathematica Book* (3rd edn). Wolfram Media, Cambridge University Press: New York/Champaign, IL, 1996.
26. Cotta RM, Mikhailov MD. *Heat Conduction—Lumped Analysis*, *Integral Transforms*, *Symbolic Computation*. Wiley-Interscience: New York, 1997.
27. Alves LSB, Cotta RM. Transient natural convection inside porous cavities—hybrid numerical–analytical solution and mixed symbolic–numerical computation. *Numerical Heat Transfer*, *Part A—Applications*, in press.

